Available online at www.sciencedirect.com
SCIENCE DIRECT®
Journal of Catalysis 220 (2003) 3–12
JOURNAL OF CATALYSIS
www.elsevier.com/locate/jcat

Oxidation of CO on a Pt/Al_2O_3 catalyst: from the surface elementary steps to light-off tests IV. Kinetic study of the reduction by CO of strongly adsorbed oxygen species

Abdennour Bourane and Daniel Bianchi *

Laboratoire d'Application de la Chimie à l'Environnement (LACE), UMR 5634, Université Claude Bernard, Lyon-I, Bat. 303, 43 Bd du 11 Novembre 1918, 69622 Villeurbanne, France

Received 19 August 2002; revised 29 May 2003; accepted 11 June 2003

Abstract

Transient experiments using mass and FTIR spectroscopy as detectors are performed at 300 K with a reduced 2.9% Pt/Al_2O_3 catalyst to study the reduction of strongly adsorbed oxygen species (denoted O_{sads}) formed by O_2 chemisorption using several y% CO/z% Ar/He mixtures (y and z in the range 0.5–10). During the first seconds of the reaction C mass balances reveal that the CO consumption is mainly due to the formation of a strongly adsorbed CO species identified as a linear CO species (denoted L) interacting with the O_{sads} species (IR band at 2084 cm^{-1}). The evolution of the CO_2 production rate with time on stream presents different profiles according to the reaction temperature: decreasing exponential at $T_r < 273$ K and peak profiles for $T_r \geqslant 300$ K. The CO_2 production at $T_r < 273$ K is in agreement with a kinetic model considering two elementary steps: the adsorption of the L CO species without competition with O_{sads} followed by a L–H elementary step (denoted S3b): $O_{sads} + L \rightarrow CO_{2ads}$, with a rate constant $k_{3b} = \nu_{3b} \exp(-E_{3b}/RT)$ and $E_{3b} = 65$ kJ/mol at $\theta_{Osads} \approx 1$. For $T_r > 300$ K, mass transfer processes contribute to the apparent CO_2 production rate. At high θ_{Osads} values, they compete with the surface reactions for 273 K $< T_r <$ 360 K and finally dominate the CO_2 production at $T_r > 360$ K. However, kinetic studies can be performed at $T_r > 300$ K after a significant decrease in θ_{Osads} due to the increase in E_{3b}: $E_{3b} = 110$ kJ/mol at $\theta_{Osads} = 0.4$. Several conclusions of the present study are in very good agreement with the reduction of O_{sads} species on Pt single crystals using a CO molecular beam under UHV conditions.
© 2003 Elsevier Inc. All rights reserved.

Keywords: CO oxidation; Pt/Al_2O_3; Kinetic modeling; Elementary steps; Kinetic parameters

1. Introduction

It is known that the linear CO species (denoted L CO) is the main adsorbed CO species present on the surface of Pt-containing solids during the CO/O_2 reaction at low temperatures [1–5]. To understand its involvement in the rate of CO_2 production we have studied each elementary step involved in a plausible kinetic model such as Model M1:

Step S1: Formation of the L species,

$$CO_{gas} \Leftrightarrow L$$

Step S2: Dissociative chemisorption of oxygen,

$$O_{2gas} \Leftrightarrow 2O_{ads}$$

Step S3: Oxidation of the L species,

$$L + O_{ads} \rightarrow CO_{2ads}$$

Step S4: Desorption of CO_2,

$$CO_{2ads} \rightarrow CO_{2gas}.$$

Step S1 has been previously studied by FTIR spectroscopy determining (a) the coverage of the L CO species under adsorption equilibrium [6–8] and (b) its heat of adsorption at several coverages [6–8]. The kinetic parameters of steps S2 and S3 have been determined studying the isothermal oxidation of the L CO species with several x%

* Corresponding author.
E-mail address: daniel.bianchi@univ-lyon1.fr (D. Bianchi).

0021-9517/$ – see front matter © 2003 Elsevier Inc. All rights reserved.
doi:10.1016/S0021-9517(03)00267-7

O_2/He mixtures [9,10]. It has been shown that the oxygen species involved in step S3 is weakly adsorbed (denoted O_{wads}) and is formed without competition with the L CO species by the dissociation of O_2 [9,10]. Moreover, studying the oxidation of the L CO species by experiments in the transient regime with a mass spectrometer as a detector it has been observed that a strongly adsorbed oxygen species (denoted O_{sads}) is formed during the removal of L CO species by step S3 leading to a situation where L CO and O_{sads} species can be simultaneously present on the Pt surface [10] without reaction. However, L CO and O_{sads} may react to produce CO_2 during a TPSR (temperature-programmed surface reaction) procedure according to a surface elementary step (denoted S3a) with a rate significantly lower than that of step S3 under our experimental conditions [10]. Moreover, O_2 chemisorption on a freshly reduced Pt surface only forms O_{sads} species (no O_{wads} species) with a heat of adsorption higher than that of the L CO species at the same coverage: i.e., at full coverage of a freshly reduced Pt surface the heats of adsorption of O_{sads} and L CO are 175 and 110 kJ/mol [10], respectively. In the present study the reduction by CO of the O_{sads} species formed by adsorption of O_2 on a reduced Pt/Al_2O_3 catalyst is studied by experiments in the transient regime in order to determine the kinetic parameters of the L–H elementary step which controls the rate of the CO_2 production at high coverages of the O_{sads} species (denoted θ_{Osads}).

2. Experimental

The 2.9% Pt/Al_2O_3 catalyst (in wt%, γ-Al_2O_3, BET area 100 m^2/g, incipient wetness method, aqueous solution of H_2PtCl_6, xH_2O) was the same as that used and characterized in previous studies [6–10]. After the reduction of the solid in a flow (100 cm^3/min) of pure H_2 at 713 K according to a procedure previously described [6–8,10], the Pt dispersion of a fresh catalyst was $D = 0.85$ [6–8]. This dispersion decreased to 0.5–0.6 after a stabilization pretreatment in 1% CO/He at 713 K [10] followed by O_2 and then H_2 treatment of the solid.

The experiments in the transient regime with a mass spectrometer as a detector have been run with an analytical system previously described [10]. Mainly, various valves allowed us to perform switches between regulated gas flows (1 atm total pressure), which passed through the catalyst (powder, $W \approx 0.2$–0.4 g) contained in a quartz microreactor. A small thermocouple (K type, $\phi = 0.25$ mm) was inserted in the catalyst powder. A quadrupole mass spectrometer permitted the determination of the composition (molar fractions) of the gas mixture at the outlet of the reactor during a switch, after a calibration procedure. The reduction of the O_{sads} species by CO was studied according to the following procedure: after the reduction of the stabilized catalyst in pure H_2 at 713 K the solid was cooled in He to 300 K and then O_2 was adsorbed performing the switch He → 2% O_2/z% Ar/He (100 cm^3/min, z in the range 2–4) during t_a. After a short (60 s) helium purge, the reactor is either heated or cooled to the reaction temperature T_r (range 220–600 K) and a new switch was performed: He → x% CO/z% Ar/He (100 cm^3/min, x in the range 0.5–4) during a time t_r while the gas composition at the outlet of the reactor was determined with the mass spectrometer. The results were mainly obtained after several cycles of reduction of the O_{sads} species/oxidation of the L CO species (denoted R/O cycles) repeating the following switches: He → 2% O_2/z% Ar/He → He → x% CO/z% Ar/He → He. Similar experiments have been performed by several authors on various noble metal-supported catalysts [11–17]. However, the main contribution of the present study in line with [10] is that the evolution of the gas molar fractions during the transient experiments is as follows: (a) exploited by C and O mass balances as in an early study of Bennett et al. [18] and (b) supported by kinetic models as previously performed for the oxidation of the L CO species [10] to determine the kinetic parameters of the surface elementary steps.

The evolution of the coverage of the Pt surface by the adsorbed CO species during the O_{sads} reduction has been studied by FTIR spectroscopy as in [9] by using a small internal volume stainless-steel IR cell (transmission mode, resolution 4 cm^{-1}) described elsewhere [6]. After adsorption of O_2 at 300 K on a pellet (weight in the range 40–80 mg) of the reduced stabilized Pt/Al_2O_3 catalyst followed by a short purge in He, the FTIR spectra of the adsorbed species were recorded during the switch He → 1% CO/He with a 200 cm^3/min flow rate.

3. Results and discussion

The O_{sads} species formed by O_2 chemisorption on the reduced Pt/Al_2O_3 catalyst desorbs in helium at $T > 820$ K with an activation energy of desorption of 175 kJ/mol at $\theta_{Osads} = 1$ [10]. At $T < 350$ K, this species only can be removed from the Pt surface by reduction as studied below with CO-containing gas mixtures. A plausible two steps mechanism can be proposed for the reduction of the O_{sads} species:

Step S1: Adsorption of CO in the presence of O_{sads},

$$CO_{gas} \Leftrightarrow CO_{ads},$$

with k_a and k_d the rate constants of adsorption and desorption, respectively.

Step S3b: Oxidation of the O_{sads} species according to a L–H step,

$$CO_{ads} + O_{sads} \rightarrow CO_{2ads},$$

with k_{3b} and E_{3b} the rate constant and the activation energy, respectively. The desorption of CO_{2ads} is fast [19] leading to a very low coverage in CO_{2ads}. To characterize this mechanism the following points have been studied: (a) the structure

of the CO_{ads} species and its heat of adsorption in the presence of O_{sads}, (b) the competitive chemisorption between the two adsorbed species, and (c) the values of k_{3b} and E_{3b} at several O_{sads} coverage (denoted θ_{Osads}).

3.1. FTIR study of the reduction of O_{sads}

After adsorption of O_2 at 300 K on Pt/Al_2O_3 using a switch He → 2% O_2/He ($t_a = 3$ min) followed by a short helium purge, the O_{sads} species are reduced during the switch He → 1% CO/He (200 cm^3/min). Fig. 1 shows the evolution of the FTIR spectra with the duration t_r of the reaction. It can be observed that the IR band of a linear CO species is immediately detected at 2084 cm^{-1} ($t_r \approx 4$ s) and that its intensity strongly increases for $t_r < 20$ s. For longer time on stream the intensity slightly increases while the IR band shifts to lower wavenumbers (2082 cm^{-1}). Small IR bands (not shown) due to multibound CO species [8] are also detected in the range 1950–1750 cm^{-1} for $t_r > 20$ s. The same experiment performed on the reduced Pt/Al_2O_3 solid (without O_{sads} species) leads to similar results: the IR band (detected at 2070 cm^{-1} [6,8]) increases for ≈ 20 s. This indicates that the presence of O_{sads} species does not modify strongly the net CO adsorption rate. The higher position of the IR band of the L CO species in Fig. 1 (as compared to a Pt-reduced surface: 2070 cm^{-1}) is due to the presence of O_{sads} [20,21]. The fact that the IR band is still detected at 2082 cm^{-1} after long time on stream (while the gas-phase analysis reveals a CO_2 production as shown below) indicates that a fraction of the O_{sads} species remains on the surface. According to Fig. 1 the L CO species interacting with the O_{sads} species, which dominates the CO adsorption, can be considered as the adsorbed intermediate species involved in step S3b. Note that in [10] studying the oxidation of L CO species with O_2, the reaction between L CO and O_{sads} species (O_{sads} adsorbed in parallel to the removal of the L CO species) has been denoted S3a. In the present study, the same reaction is denoted S3b because for high θ_{Osads} values the reaction rate is strongly higher (S3a and S3b correspond to the same reaction at low and high θ_{Osads} values).

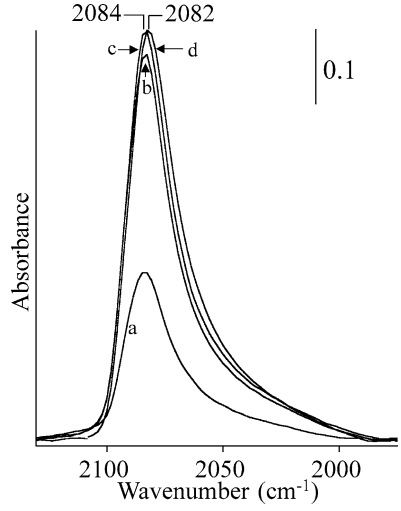

Fig. 1. FTIR spectra in the course of the reduction of O_{sads} species on Pt/Al_2O_3 using 1% CO/He at 300 K: (a–d) 4, 8, 16 and 230 s.

3.2. Mass spectroscopy study of the reduction of the O_{sads} species by CO

3.2.1. Isothermal reduction at 300 K and temperature-programmed experiments

Fig. 2A shows the evolution at 300 K of the composition of the gas mixture at the outlet of the reactor during a switch He → 2% O_2/4% Ar/He on the freshly reduced Pt/Al_2O_3 solid. It can be observed that the O_2 signal (curve b) is 0 during several seconds due to the formation of the O_{sads} species. Curves a and b allow us to determine the amount of adsorbed oxygen QAO = 70 μmol O/g [10]. After a purge in He indicating the absence of reversible chemisorption (no weakly adsorbed oxygen species) at 300 K [10], Part B in Fig. 2 gives the evolution of the molar fractions during a switch He → 2% CO/4% Ar/He. There is no O_2 production indicating the absence of competition between CO and O_{sads} in agreement with their respective heats of adsorption. The O_{sads} species are only removed from the surface by reduction with CO. The CO_2 molar fraction (Fig. 2B, curve d) provides the apparent CO_2 production rate (μmol/(g_{cat} s)) during the isothermal reduction,

$$RCO2_{ir} = (\text{curve d}) \times \frac{F}{W}, \quad (1)$$

where F and W are the gas molar flow rate and the weight of the catalyst, respectively. The integration of $RCO2_{ir}$ (maximum characterized by $RCO2_{irm}$ and t_m) for the duration of the isothermal reduction provides the total amount of the CO_2 production: $QCO2_{ir} = 40$ μmol/g. $QCO2_{ir}$ is lower

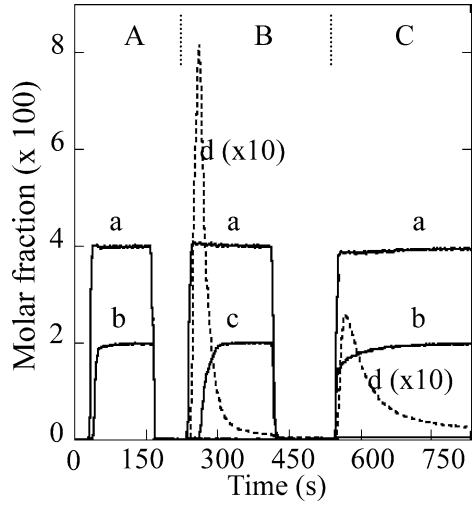

Fig. 2. Molar fractions during several switches at 300 K on Pt/Al_2O_3: (a) argon, (b) O_2, (c) CO, and (d) CO_2. (Part A) Adsorption of O_2 on the freshly reduced solid using 2%O_2/4% Ar/He. (Part B) Reduction of the O_{sads} species using 2% CO/4% Ar/He. (Part C) Oxidation of the L CO species using 2% O_2/4% Ar/He.

than QAO because $RCO2_{ir}$ strongly decreases with time on stream due to the decrease in θ_{Osads}. At 300 K after several minutes of reduction a significant fraction of the O_{sads} species is left on the Pt surface. This explains that the IR band of the L CO species in Fig. 1 remains at a position (2082 cm^{-1}) higher than that on a freshly reduced Pt surface (2070 cm^{-1}). The O_{sads} species which are left on the surface after $t_r \approx 2$ min can be removed by temperature-programmed reduction (TPR) as shown below. Moreover, during the first R/O cycle a fraction of the CO_2 production is strongly adsorbed as carbonate by the Al_2O_3 support [10] imposing to perform exploitable C mass balances after several R/O cycles to saturate the support. The CO consumption during the reduction using curves a and c in Fig. 2B is higher than $QCO2_{ir}$ because adsorbed CO species are formed during the O_{sads} reduction (formation of the L CO species). For instance, in Fig. 2B the CO signal is 0 during the first seconds of the switch while the CO_2 production increases to a maximum at $t_{rm} = 18$ s (from the appearance of Ar). Li et al. [22] have made similar observations on a Pt/SiO_2 catalyst: CO_2 is detected before CO. This delay between CO and CO_2 is due to the fact that CO is involved in both the CO_2 production and the CO adsorption to form the L CO species (Fig. 1). After a helium purge the introduction of 2% O_2/4% Ar/He (Fig. 2C) leads to the oxidation of the L CO species as previously studied [10]. At the opposite of Fig. 2A there is no delay between the Ar and O_2 molar fractions in Fig. 2C because the oxygen species involved in the L CO oxidation is weakly adsorbed [10]. Fig. 2B and C show similarly to previous results [10] that RCO2 is lower during the oxidation step (Fig. 2C) than during the reduction step for the same partial pressures of O_2 and CO. This has been observed in early studies by Cutlip and co-workers [23,24] and the authors have shown that periodic switches between CO and O_2 can lead to a higher CO_2 production (time average) than at steady state.

Figs. 3A and B show the CO_2 production (a) during a reduction at 300 K ($QCO2_r = 43$ μmol/g) with 2% CO/4% Ar/He after several R/O cycles (saturation of the support by CO_2) and (b) during a TPR between 300 and ≈ 370 K (26 μmol/g) with a flow of CO/Ar/He, respectively. The CO_2 production during the TPR corresponds to the overlap of the reduction of O_{sads} species remaining on the surface and the desorption of the carbonate species from the support: ≈ 6 μmol CO_2/g [10]. The total CO_2 production linked to the O_{sads} species: ≈ (43 + 20) = 63 μmol/g is in reasonable agreement with the amount of adsorbed oxygen: QAO = 70 μmol/g. The difference may indicate that there is a reconstruction of the Pt surface during the previous R/O cycles that slightly decreases the amount of O_{sads} species.

3.2.2. Impact of the experimental conditions on the isothermal reduction

This impact must be determined to fix the experimental conditions allowing to determination of the kinetic parameters of step S3b from the CO_2 production. The effect of the

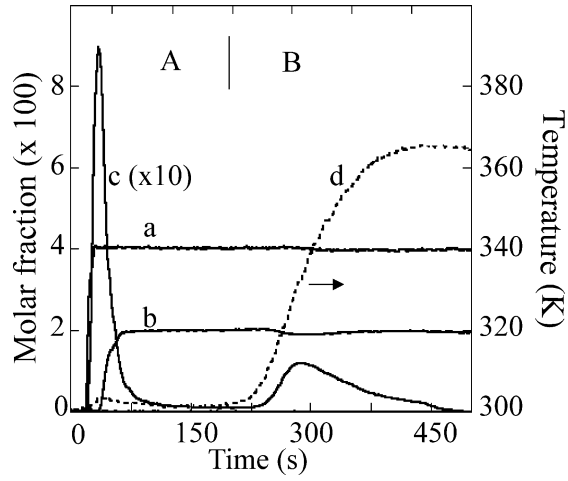

Fig. 3. Isothermal (Part A) and temperature-programmed (Part B) reduction of O_{sads} species on Pt/Al_2O_3: (a) Ar, (b) CO, and (c) CO_2 and (d) temperature of the catalyst.

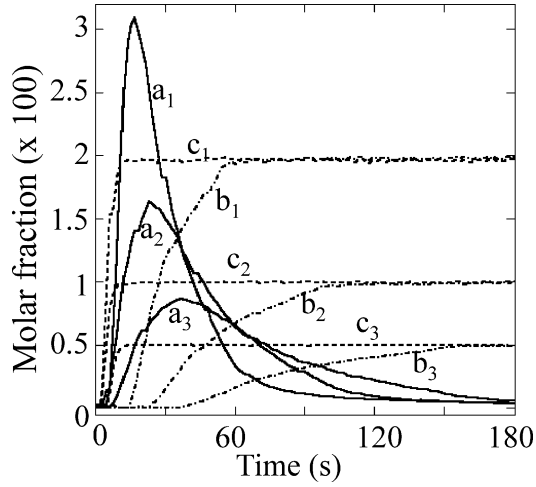

Fig. 4. Evolutions of the gas molar fractions during the reduction at 300 K of the O_{sads} species on Pt/Al_2O_3 using several x% CO/x% Ar/He mixtures (flow rate 100 cm^3/min): (a_i) CO_2 (×4); (b_i) CO; (c_i) Ar with subscripts 1, 2, 3 for $x = 2$, 1, and 0.5, respectively.

CO partial pressure (denoted P_{CO}) on $RCO2_{ir}$ at 300 K has been studied during consecutive R/O cycles using several y% CO/z% Ar/He mixtures. Fig. 4 gives the molar fractions of CO_2 (curves a_1, a_2, a_3), CO (curves b_1, b_2, b_3), and Ar (curve c_1, c_2, c_3) for $y = z = 2$, 1, and 0.5, respectively. It can be observed that (a) the increase in P_{CO} increases $RCO2_{irm}$ and decreases t_{rm} without changing significantly $QCO2_{ir}$ and (b) the CO conversion is very high during several seconds. Fig. 5 shows that the increase in T_r (> 300 K) using 100 cm^3/min of 1% CO/1% Ar/He leads to a modification of the $RCO2_{ir}$ profile which evolves from a peak with a well-defined maximum (Figs. 5a and 5b) to a peak with a plateau at high temperatures (Fig. 5c). Moreover, $QCO2_{ir}$ increases with the increase in T_r because according to the TPR results (Fig. 3) more O_{sads} species can be oxidized. We have observed (results not shown) a similar apparent CO_2 production rate in the range 353–673 K, indicating clearly

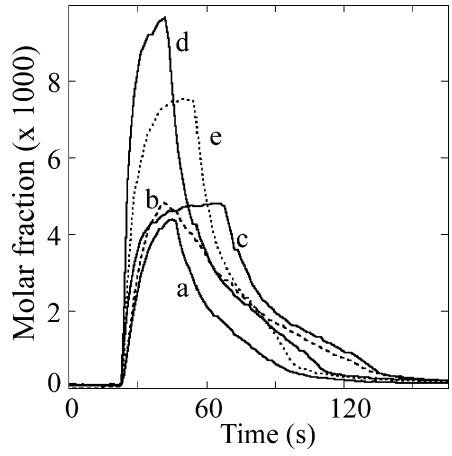

Fig. 5. CO_2 production during the reduction of O_{sads} species on Pt/Al_2O_3 for several experimental conditions: (a–c) 100 cm^3/min of 1% CO/1% Ar/He at 305, 328, and 353 K, respectively; (d) 200 cm^3/min of 1% CO/1% Ar/He at 353 K; (e) 100 cm^3/min of 1.6% CO/1% Ar/He at 353 K.

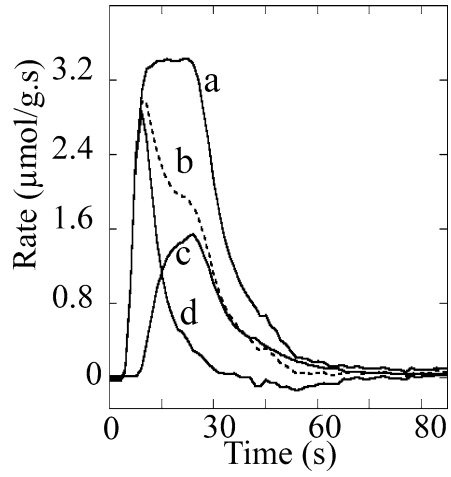

Fig. 6. Evolution of the rates of several processes during the isothermal reduction (300 K) of the O_{sads} species on Pt/Al_2O_3 using 0.5% CO/0.5% Ar/He: (a) rate of CO consumption (RCOC); (b) net CO adsorption rate (RCO_{ads}); (c) rate of CO_2 formation ($RCO2_r$); (d) net rate CO adsorption before CO_2 production.

that there is a mass transfer limitation in agreement with the conclusions of Li et al. [22] for similar experiments on Pt/SiO_2. This is confirmed considering the impact of the other experimental conditions on the $RCO2_{ir} = f(t_r)$ profile. For instance, at $T = 353$ K the increase in the flow rate from 100 to 200 cm^3/min for $P_{CO} = 1000$ Pa increases $RCO2_{irm}$ by 2 (compare Figs. 5c and 5d). Similarly, the increase in P_{CO} from 1000 to 1600 Pa at constant flow rate increases $RCO2_{irm}$ by the same factor (compare Figs. 5c and 5e) while the $QCO2_{ir}$ values are equal (58 µmol/g). For high θ_{Osads} values, the influence of P_{CO} at 300 K on the CO_2 production (Fig. 4) comes from the competition between surface reactions and mass transfer processes. At $T_r > 350$ K, these processes control the CO_2 production (CO_2 peak with a plateau) while for 300 K $< T_r <$ 350 K they compete with the surface reactions. For the evaluation of the kinetic parameters of step S3b the impact of the mass transfer processes must be negligible by using experimental conditions leading to a low CO conversion (< 5%, differential microreactor). At high θ_{Osads} values, this imposes the use of low reaction temperatures ($T_r < 300$ K) to decrease k_3 and for $T_r > 300$ K only the data in the final part of the transient (Figs. 4 and 5) must be exploited. However, the experiments at $T_r = 300$ K can be used to perform C mass balances to follow the evolution of the Pt surface during the reaction.

3.3. Evolution of the Pt surface composition during the reduction of the O_{sads} species

After several R/O cycles, C mass balances during the isothermal reduction (300 K) of O_{sads} (Fig. 4) according to a procedure similar to that used in [10] allow determination of the apparent rates of several processes at the Pt surface. For instance, $RCO2_{ir}$ for 0.5% CO/0.5% Ar/He is given by expression (1) using curve a_3 in Fig. 4. The evolution of the total CO consumption rate RCOC (reduction of the O_{sads} species and CO adsorption) with the duration of the reduction is given by

$$\mathrm{RCOC} = (\mathrm{curve}\, c_3 - \mathrm{curve}\, b_3)\frac{F}{W}. \tag{2}$$

The total amount of CO consumption QCOC is obtained integrating RCOC. The evolution of the net apparent CO adsorption rate RCO_{ads} with t_r is given by

$$\mathrm{RCO_{ads}} = \mathrm{RCOC} - \mathrm{RCO2_{ir}}. \tag{3}$$

The integration of RCO_{ads} provides QACO, the total amount of adsorbed CO during the isothermal reduction. Fig. 6 shows the evolutions of RCOC, RCO_{ads}, and $RCO2_{ir}$ curves a, b, and c, respectively, in the course of the reduction at 300 K with $P_{CO} = 500$ Pa. It can be observed that in the first seconds of the reduction curves a and b are overlapped, indicating that the CO consumption is due to the CO adsorption (CO is adsorbed without a significant removal of the O_{sads} species). This indicates that a strongly adsorbed CO species ($P_{CO} \approx 0$ during the first seconds) is formed without any competition with the O_{sads} species in agreement with the strong increase in the IR band of the L CO species in Fig. 1. During the final part of the reduction ($t_r > 20$ s) there is roughly an equality between RCO_{ads} (curve b) and $RCO2_{ir}$ (curve c) because strongly adsorbed CO species are formed in parallel with the removal of the O_{sads} species. Note that during the L CO oxidation [10], the situation is clearly different because O_2 and Ar molar fractions increase simultaneously (see also Fig. 2) due to the formation of the O_{wads} species. It has been verified that there is no significant CO adsorption at 300 K on the Al_2O_3 support alone treated at 713 K as the Pt/Al_2O_3 catalyst and saturated by CO_2 at 300 K (γ-Al_2O_3 adsorbs significantly CO only after a treatment at 1073 K [25]). Curve d in Fig. 6 gives

RCO_{ads}–$RCO2_{ir}$ showing that CO is adsorbed in the first seconds of the switch He → CO/Ar/He without removal of O_{sads}. This is in agreement with the observations on Pt single crystals that indicate that preadsorbed CO inhibits the dissociative chemisorption of oxygen whereas a preadsorbed oxygen layer only slightly affects the sticking probability for CO [26,27]. Xu et al. [27] have shown that 0.55 ML of CO can be adsorbed at saturation on a clean Pt(111) surface while this amount only decreases to 0.4 ML on the surface saturated with O_{sads} (0.25 ML). The $QCO2_{ir}$ values for the reduction of O_{sads} with $P_{CO} = 1$ kPa indicate that θ_{Osads} decreases to steady-state values of 0.6 and 0.4 at 300 and 353 K, respectively. These remaining O_{sads} fractions are due to the decrease in k_{3b} associated with the decrease in θ_{Osads}.

3.4. Determination of the kinetic parameters of step S3b

According to step S3b, the rates of disappearance of the O_{sads} species and of the CO_2 production expressed as a turnover number (s^{-1}) are given by

$$-\frac{d\theta_{Osads}}{dt} = k_{3b}\theta_{Osads}\theta_L. \quad (4)$$

Considering (a) steps S1 and S3b and (b) the absence of competition between CO_{sads} and O_{sads}, the evolution of the coverage of the L CO species (θ_L) is given by

$$\frac{d\theta_L}{dt} = R_a - R_d - R_{CO_2} = k_a P_{CO}(1-\theta_L) - k_d\theta_L - k_{3b}\theta_{Osads}\theta_L. \quad (5)$$

where R_a and R_d are the rates of adsorption and desorption of the L CO species, respectively. Assuming that θ_L is constant during the reduction of the O_{sads} species, expression (4) leads to $\ln\theta_{Osads} = -k_{3b}\theta_L t$, showing that k_{3b} can be obtained from the slope of the experimental curves $\ln\theta_{Osads} = f(t)$ at constant T_r. Expression (5) permits to specify the experimental conditions leading to a constant θ_L value during the reaction. This expression can be simplified assuming that the heat of adsorption of L CO species is high enough to consider $k_d\,\theta_L \ll k_{3b}\theta_{Osads}\theta_L$ (this assumption is experimentally justified below). During the first seconds of the switch He → x% CO/y% Ar/He and whatever the reaction temperature: R_a is very high and $d\theta_L/dt > 0$. The duration under CO/Ar/He to obtain $d\theta_L/dt = 0$ depends on (a) the $k_a\ P_{CO}$ values and (b) the mass transfer processes at $T > 300$ K. To prevent these impacts and to maintain θ_L constant during the reaction the following experimental conditions must be used at high θ_{Osads}: a high CO partial pressure (to favor the CO adsorption) and a low T_r value (to decrease R_{CO_2}). Fig. 7A gives the evolution of the CO_2 production with t_r for three temperatures < 273 K using 100 cm^3/min of 10% CO/2% Ar/He mixture. It has been verified that for $T_r < 273$ K, the experimental parameters such as $P_{CO} > 5$ kPa and flow rates (higher than 100 cm^3/min) have no impact on the rate of the CO_2 production at the opposite of Figs. 4 and 5. From a curve $RCO2_{ir} = f(t)$ at a constant T_r value, the evolution of

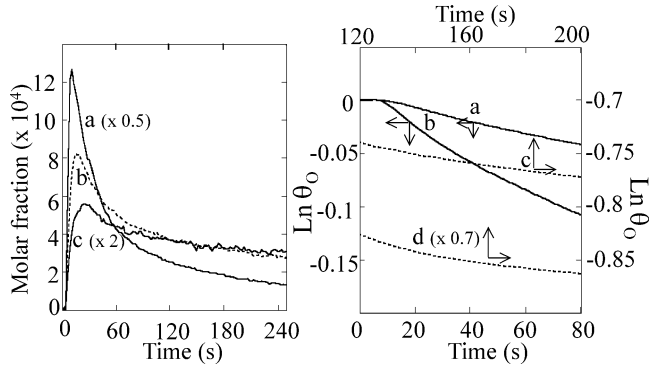

Fig. 7. Determination of the activation energy E_{3b} of the L–H step S3b on Pt/Al_2O_3. (Part A) CO_2 production at low temperatures with 100 cm^3/min of 10% CO/4% Ar/He: (a) 235 K, (b) 220 K, and (c) 213 K. (Part B) $\ln(\theta_{Osads}) = f(t_r)$ at several temperatures: (a–d) 213, 220, 321, and 353 K.

$\theta_{Osads}(t)$ is given by

$$\theta_{Osads}(t) = 1 - \frac{\int_0^t RCO2_{ir}\,dt}{QAO}, \quad \text{where } 0 \leqslant t \leqslant t_r. \quad (6)$$

Curves a and b in Fig. 7B gives $\ln(\theta_{Osads}) = f(t)$ for $T_r =$ 213 and 223 K, respectively. They correspond to straight lines for limited duration of the reaction due to the decrease in k_{3b} with the decrease in θ_{Osads}. The slopes for a decrease in θ_{Osads} from 1 to 0.94 lead to k_{3b} at $\theta_{Osads} \approx 1$ which provides the activation energy: $E_{3b} \approx 65$ kJ/mol at $\theta_{Osads} \approx 1$ assuming a preexponential factor of 10^{13} s^{-1} for a L–H elementary step. Simple calculations assuming E_{3b} constant with θ_{Osads} show that at 300 K the coverage of the O_{sads} species must decrease to 0 in contradiction with the experimental observations. This is due to the strong increase in E_{3b} with the decrease in θ_{Osads} as confirmed by the following experiments. At $T_r > 300$ K, to prevent the impact of mass transfer processes, θ_{Osads} must be decreased by reduction with CO to obtain low k_{3b} values. From experiments similar to those in Fig. 4, the $RCO2_{ir}$ values after a long reaction duration (CO conversion < 10%) allow us using expression (6) to obtain curves c and d in Fig. 7B which give $\ln\theta_{Osads} = f(t)$ at T_r= 321 and 353 K for θ_{Osads} values of 0.47 and 0.39, respectively. The slopes provide k_{3b} and then E_{3b}: $E_{3b} \approx 108$ kJ/mol at $\theta_{Osads} \approx 0.47$ and $E_{3b} \approx 110$ kJ/mol at $\theta_{Osads} \approx 0.39$. The comparison with $E_{3b} \approx 65$ kJ/mol at $\theta_{Osads} \approx 1$ clearly shows that E_{3b} increases with the decrease in θ_{Osads}. This justifies the formalism S3a and S3b used in [10] and in the present study to denote the surface reaction between L CO and O_{sads} species: S3a and S3b correspond to the same L–H step at low and high θ_{Osads} values, respectively.

3.5. Characterizations of the L CO species formed in the presence of O_{sads}

This L CO species with an IR band at 2084 cm^{-1} (2070 cm^{-1} on freshly reduced Pt surface) has been characterized (a) by determining its amount on a O_{sads}-saturated

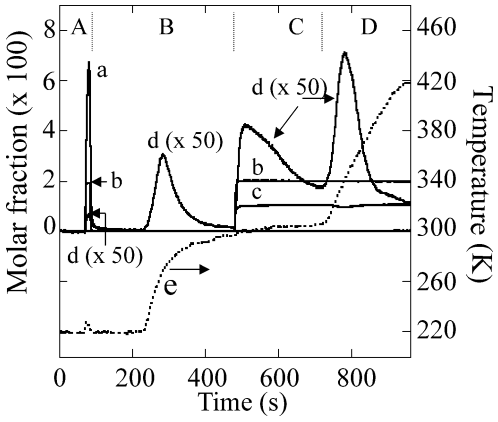

Fig. 8. Evolution of the molar fractions of the gases during several transient experiments after adsorption of O_2 at 300 K on Pt/Al_2O_3: (a) CO, (b) Ar, (c) O_2, and (d) CO_2 and (e) temperature. (A) Introduction of CO/Ar/He at 223 K; (B) isothermal desorption in helium followed by a TPD up to 300 K; (C) introduction of O_2/Ar/He at 300 K; (D) TPO.

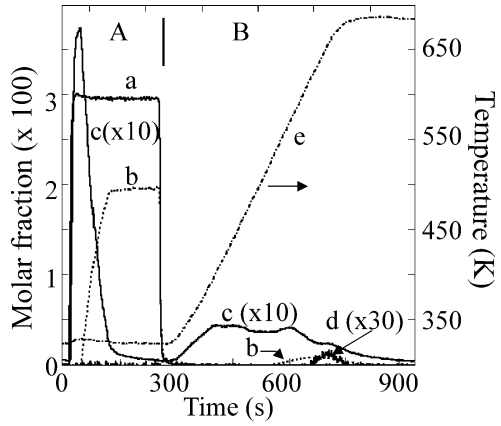

Fig. 9. Evolution of the molar fractions of the gases during a TPD after reduction of the O_{sads} species at 323 K: (a) Ar, (b) CO, (c) CO_2, and (d) H_2 and (e) temperature. (Part A) Isothermal reduction of O_{sads}. (Part B) TPD in helium.

Pt surface and (b) by comparing its heat of adsorption to the L CO species formed on a O-free Pt surface. At $T_r = 223$ K, the rate of step S3b is very low and the saturation of the surface by the L CO species can be obtained without the significant removal of the O_{sads} species. This allows us to determine the highest amount of CO which can be adsorbed on a surface precovered by O_{sads} according to the following experiment: after the adsorption of O_{sads} at 300 K on Pt/Al_2O_3 using a switch He → 1% O_2/He, the solid is cooled in helium to 223 K. Then a switch He → 10% CO/Ar/He (flow rate 100 cm^3/min) is performed during ≈ 20 s (Fig. 8A) to rapidly saturate the surface without the removal of a large amount of O_{sads} species (small CO_2 peak of 0.5 μmol/g in Fig. 8A). An accurate C mass balance to evaluate $QACO_{ir}$ cannot be performed with the data in Fig. 8A due to the large CO molar fraction. A reversible CO chemisorption is detected in Fig. 8B during the switch CO/Ar/He → He, 15 μmol of CO/g, also observed on a sample of pure Al_2O_3 support. This adsorption explains that the CO molar fraction in Fig. 8A is < 0.1 before the He switch. After the total CO desorption from the support, the temperature is increased in helium up to 300 K (Fig. 8B, TPSR between O_{sads} and L CO species) leading to a CO_2 peak with a maximum at 267 K: 12 μmol/g. There is no CO desorption during the TPSR justifying the approximation: $k_d\ \theta_L \ll k_{3b}\theta_{Osads}\theta_L$. At 300 K, a 1% O_2/2% Ar/He mixture is introduced to oxidize [10] the remaining L CO species (Fig. 8C), $QCO_2 = 36$ μmol/g, and then the temperature is increased (Fig. 8D) in the presence of O_2 (TPO) leading to a CO_2 peak, 39 μmol/g. A fraction of this last amount is probably due to the desorption of CO_2 from the support: ≈ 6 μmol/g [10]. The total CO_2 production in Fig. 8 gives the amount of CO coadsorbed with the O_{sads} species at 223 K: QACO ≈ 80 μmol/g. This indicates clearly that on a Pt surface saturated with O_{sads} species, the amount of L CO species at full coverage is as high as that on a freshly reduced Pt surface. This conclusion is in good agreement with that of Xu et al. [27] who have shown that 0.55 ML of CO can be adsorbed at saturation on a clean Pt(111) surface while this amount only decreases to 0.4 ML on the surface saturated with O_{sads} (0.25 ML).

Fig. 8B shows that the L CO species preferentially reacts with O_{sads} to form CO_2 (it does not desorb as CO). This justifies the approximation $k_d\ \theta_L \ll k_{3b}\theta_{Osads}\theta_L$ and indicates a high heat of adsorption for the L CO species at $\theta_L = 1$. These conclusions are also true for lower θ_{Osads} values as shown in Fig. 9. After adsorption of O_2 at 300 K, the reduction of the O_{sads} species is performed at 323 K with 2% CO/3% Ar/He (Fig. 9A) (to decrease significantly θ_{Osads}) then after a purge in helium the temperature is increased up to 680 K (Fig. 9B, TPSR/TPD). It can be observed in Fig. 9B that for $T < \approx 500$ K only CO_2 is detected due to step S3b. At $T > 500$ K, CO and CO_2 are detected due to several processes. The CO_2 production can be due to (a) the CO disproportionation on the Pt particles and (b) the decomposition/desorption of the formiate and carbonate species formed on the Al_2O_3 support [32]. The CO production can be due to (a) the CO desorption from Pt particles and (b) the desorption/decomposition of formiate species on the support (the H_2 production (curve d) comes from the formiate species [32]). Fig. 9 clearly shows that the L CO species coadsorbed with O_{sads} at $\theta_{Osads} < 1$ preferentially reacts to form CO_2 justifying the assumption $k_d\ \theta_L \ll k_{3b}\theta_{Osads}\theta_L$. The L CO species only desorbs from the surface at high temperatures after the total removal of the O_{sads} species. It seems that the heat of adsorption of the L CO species is not strongly modified by the presence of O_{sads} species.

3.6. Comparison of the present results with UHV studies on Pt single crystals

This comparison reveals that the observations during the reduction of the O_{sads} by CO either on single crystals using a molecular beam [19,26,27,29] or on the present Pt-supported particles are very similar. For instance, for 300 K > T_r > 400 K, Zaera et al. [29] observe on Pt(111) saturated

with O_{sads} (denoted O–Pt(111)) that the rate of the CO_2 production rapidly increases when the CO beam is turned on, before the removal of large amount of O_{sads} species. They conclude in agreement with [26] that the reaction between O_{sads} and CO proceeds according to a L–H elementary step via a CO species adsorbed without competition with the O_{sads} species. Moreover, Zaera et al. [29] observe in agreement with Campbell et al. [26] that CO can be adsorbed at $T < 300$ K on O–Pt(111) ($\theta_O = 0.25$ ML) (a) without significant CO_2 production due to the low rate of the L–H step, (b) with an initial sticking coefficient for CO (≈ 0.8) and a CO saturation coverage (≈ 0.4 ML) similar to those on the clean Pt(111) surface. This is in very good agreement with our observations in Fig. 8 which shows that large amounts of CO (≈ 80 μmol/g) can be adsorbed in the presence of O_{sads} species. This absence of competition agrees with the conclusions of Szabo et al. [28] who have shown on Pt(111) that CO can be adsorbed on top sites at the middle of the triangle formed by oxygen atoms. The absence of CO_2 production at $T < 300$ K on O–Pt(111) [29] indicates that the adsorbed CO and O species are slightly less reactive than on the present Pt/Al_2O_3 solid (CO_2 is detected at $T = 223$ K in Fig. 7). This difference is probably due to the higher reactivity of the step/defect sites (mainly present on Pt/Al_2O_3) as compared to the terrace sites of the Pt(111) surface [29]. Moreover, Xu et al. [27] using RAIRS show that the large amount of CO on O–Pt(111) gives an IR band at 2107 cm^{-1} ascribed to a L CO species on terrace sites interacting with O_{sads} species (IR band at 2103 cm^{-1} on a clean Pt(111) surface). This agrees very well with the IR band at 2084 cm^{-1} in Fig. 1 as compared to 2070 cm^{-1} on a freshly reduced Pt/Al_2O_3 catalyst [6–8].

The kinetic parameters for step S3b are also in good agreement with those determined for the L–H step on Pt single crystals. For instance, expressions (4) and (5) consider that the adsorbed species are well intermixed during the reaction (mean field approximation [30]) and that the reduction reaction is not controlled by the island formation. Zaera et al. [29] conclude similarly that their results disagree with the idea that the surface reaction takes place preferentially at the boundaries of oxygen islands. The increase in E_{3b} with the decrease θ_{Osads} is also in agreement with single crystal studies. On O–Pt(111) for T_r in the range 300–340 K, it is observed [29] that $RCO2_{ir}$ decreases with the duration t_r of the reaction to a very low value while a significant amount of O_{sads} species remains on the surface. However, a TPSR experiment leads to a CO_2 production (similarly to Figs. 3, 8B, and 9B) due to the reaction of the remaining O_{sads} and the coadsorbed L CO species (the lower is T_r, the higher is the CO_2 production during the TPSR) [29]. Zaera et al. [29] consider that this is due to an increase in the activation energy of the elementary L–H step with the decrease in θ_{Oads} and Campbell et al. [26] have determined that this activation energy increases from 47 to 100 kJ/mol at high and low θ_{Osads} values, respectively. These values are similar to those of E_{3b} determined in the present study: 65 and 110 kJ/mol at $\theta_{Osads} \approx 1$ and 0.39, respectively. Wartnaby et al. [31] using single crystal calorimetry mention a dramatic decrease in the reduction rate with failing oxygen coverage for reduction of O–Pt(110) by CO pulses. In line with the view of Campbell et al. [26], the increase in E_{3b} can be quantitatively linked, according to a classical potential energy diagram for the catalytic mechanism, to the increase in the heats of adsorption of the O_{sads} species with the decrease in the coverage.

Experiments in Figs. 8 and 9 support the approximation: $R_d \ll R_{CO2}$ used in expression (5). This indicates that the heat of adsorption of the L CO species (E_θ) remains high in the presence of O_{sads} (the E_θ values can not be determined as in [6–8] due to the preferential reaction of L CO with O_{sads}). However, this conclusion is in line with Wartnaby et al. [31] who have measured by single crystal calorimetry the excess energy (9 kJ/mol) removed by the desorbing CO_2 molecules during the reduction of O–Pt(110) by CO (as compared to 52 kJ/mol for the CO_2 produced during the oxidation of preadsorbed L CO species by O_2). The authors indicate that the lower values during the reduction of O_{sads} species are due to the formation of strongly adsorbed CO species [31] with a heat of adsorption of 155 kJ/mol in the coverage range ≈ 0.5–0.9. Recent density functional theory calculations [33] confirm that the heat of adsorption of CO on top sites ($\theta_{CO} = 0.25$ ML) of an oxygen saturated Pt(111) surface ($\theta_O = 0.25$ ML) is very close (170 kJ/mol) to that on a clean Pt(111) surface (177 kJ/mol) at the same CO coverage. It must be noted that this last value is in very good agreement with that determined on the present reduced Pt/Al_2O_3 catalyst at $\theta = 0.25$ using FTIR spectroscopy: 183 kJ/mol [6–8].

3.7. Comparison of the present results to literature data on supported metal catalysts

Transient experiments involving switches between CO and O_2 on Pt-containing catalysts have been reviewed by Bennett [11]. For the reduction of O_{sads} by CO the experiments (either step functions or pulses) indicate that CO_2 is formed immediately (no induction period) [22,34–37]. There is an agreement to consider that the O_{sads} and CO_{ads} are adsorbed without competition [34–37]. However, the results are usually interpreted considering a weakly adsorbed CO precursor (CO_{wads}) either using a modified E–R mechanism (denoted MER in [34]) or involving a reaction at the boundaries of CO and O islands on the Pt surface [35,37]. However, Dwyer and Bennett [34] consider that in parallel to the CO_2 production via CO_{wads}, there is a classical L–H reaction between O_{sads} and a strongly adsorbed CO species formed on the sites created by the removal of O_{sads}. The MER mechanism predominates during the first seconds of the transient and as the reaction proceeds the L–H step becomes the predominating reaction mechanism [34]. It must be noted that the authors mainly perform experiments at $T_r > 300$ K when the rate

of the CO_2 production for $\theta_{Osads} \approx 1$ (Figs. 4 and 5) can be controlled by a competition between the surface reaction rates and the mass transfer processes. The impact of the CO partial pressure (Fig. 4) can be wrongly interpreted as the contribution of a CO_{wads} species. Hoebink et al. [35] have shown, in line with an early study [36], that a kinetic model considering a reaction at the boundaries of O islands via a CO_{wads} precursor can represent reasonably the $RCO_2 = f(t_r)$ profile during the transient regime. However, the authors note that this is obtained considering a CO sticking coefficient $s_o = 3 \times 10^{-5}$ that is far below the reported values on single crystals: i.e., 0.6–0.8 on O–Pt(111) [27,29]. The impact of the mass transfer processes during the transient regime of the O_{sads} reduction has been noted in an early study by Li et al. [22] who indicate (without kinetic modeling) that the CO_2 production rate of on Pt/SiO_2 at $T_r > 300$ K is limited in the initial stage of the switch He $\rightarrow x$% CO/He by the constant flux of CO into the reactor in good agreement with the present observations.

4. Conclusions

The following conclusions are derived from the present study on the reduction of strongly adsorbed oxygen species (O_{sads}) by CO on a 2.9% Pt/Al_2O_3 catalyst: (a) O_{sads} species can be reduced at $T_r > 210$ K in the presence of x% CO/He mixtures according to a L–H elementary step (step S3b, with a rate constant $k_{3b} = \nu_{3b} \exp(-E_{3b}/RT)$) involving a strongly adsorbed linear CO species interacting with O_{sads}; (b) the L CO species is formed without competition with O_{sads}; (c) at $T_r \geqslant 300$ K, the CO_2 production rate is influenced by mass transfer processes for high θ_{Osads} values, imposing to use $T_r < 273$ K to evaluate k_{3b} and E_{3b} at $\theta_{Osads} = 1$; (d) E_{3b} increases with the decrease in θ_{Osads} from 65 to 110 kJ/mol at $\theta_{Osads} = 1$ and 0.39, respectively; (e) the amount of L CO species for $\theta_{Osads} = 1$ is similar to that on a freshly reduced Pt surface, and (f) the present experimental results are in good agreement with UHV observations on Pt single crystals. In a forthcoming paper and in complement to a previous study on the CO/O_2 reaction in excess CO [38], it is shown that the kinetic parameters determined in the present study and in previous works [9,10] allow us to explain the change in the coverage of the Pt particle surface and in the TOF during light-off tests in the range 300–740 K using several 1% CO/x% O_2/He with x in the range 0.125–50.

5. Nomenclature

5.1. Amounts involved in the O_{sads} reduction

QAO total amount of adsorbed O species at 300 K on a freshly reduced solid

$QCO2_{ir}$ CO_2 formed during the isothermal reduction of O_{sads}

QCOC total amount of CO consumed during the isothermal oxidation

$QACO_{ir}$ total amount of adsorbed CO species during the isothermal reduction

5.2. Rates of processes involved in the reduction of the O_{sads} species

$RCO2_{ir}$ rate of the CO_2 production during the isothermal reduction

RCOC rate of total CO consumption

RCO_{ads} net rate of CO adsorption

R_a, R_d theoretical CO adsorption and desorption rates, respectively

R_{CO_2} theoretical rate of CO_2 production.

Acknowledgments

We acknowledge with pleasure FAURECIA Industries, Bois sur Prés, 25 550 Bavans, France, for its financial support and the MENRT (Ministère de l'Education Nationale, de la Recherche et de la Technologie) for the research fellowship of A. Bourane. D.B. dedicates the present study to the memory of Prof. J.E. Germain from Lyon University who died in December 2002.

References

[1] T.H. Lindstrom, T.T. Tsotsis, Surf. Sci. 150 (1985) 487.
[2] Y. Barshad, X. Zhou, E. Gulari, J. Catal. 94 (1985) 128.
[3] D.J. Kaul, R. Sanz, E.E. Wolf, Chem. Eng. Sci. 42 (1987) 1399.
[4] D.M. Haaland, F.L. Williams, J. Catal. 76 (1982) 450.
[5] N.W. Cant, D.E. Angove, J. Catal. 97 (1986) 36.
[6] T. Chafik, O. Dulaurent, J.L. Gass, D. Bianchi, J. Catal. 179 (1998) 503.
[7] O. Dulaurent, D. Bianchi, Appl. Catal. 196 (2000) 271.
[8] A. Bourane, O. Dulaurent, D. Bianchi, J. Catal. 196 (2000) 115.
[9] A. Bourane, D. Bianchi, J. Catal. 202 (2001) 34.
[10] A. Bourane, D. Bianchi, J. Catal. 209 (2002) 114.
[11] C.O. Bennett, Adv. Catal. 44 (2000) 329.
[12] B.N. Racine, M.J. Sally, B. Wade, R.K. Herz, J. Catal. 127 (1991) 307.
[13] M. Bowker, I.Z. Jones, R.A. Bennett, S. Poulston, Stud. Surf. Sci. Catal. 116 (1998) 431.
[14] H. Conrad, G. Ertl, J. Küppers, Surf. Sci. 76 (1978) 323.
[15] A.T. Pasteur, X.C. Guo, T. Ali, M. Gruyters, D.A. King, Surf. Sci. 366 (1996) 564.
[16] T. Matsushima, J. Catal. 55 (1978) 337.
[17] X. Zhou, E. Gulari, Langmuir 2 (1986) 709.
[18] C.O. Bennett, L.M. Laporta, M.B. Cutlip, Stud. Surf. Sci. Catal. 30 (1987) 143.
[19] T. Engel, G. Ertl, Adv. Catal. 28 (1979) 1.
[20] J. Sarkany, M. Bartok, R.D. Gonzalez, J. Catal. 81 (1983) 347.
[21] P.J. Lévy, V. Pitchon, V. Perrichon, M. Primet, M. Chevrier, C. Gauthier, J. Catal. 178 (1998) 363.
[22] Y.E. Li, D. Boecker, R.D. Gonzalez, J. Catal. 110 (1988) 319.
[23] M.B. Cutlip, AIChE J. 25 (1979) 502.
[24] M.B. Cutlip, C.J. Hawkins, D. Mukesh, W. Morton, C.N. Kenney, Chem. Eng. Commun. 22 (1983) 329.

[25] O. Dewaele, G.F. Froment, Appl. Catal. 185 (1999) 203.
[26] C.T. Campbell, G. Ertl, H. Kuipers, J. Segner, J. Chem. Phys. 73 (1980) 5862.
[27] M. Xu, J. Liu, F. Zaera, J. Chem. Phys. 104 (1996) 8825.
[28] A. Szabo, M. Kiskinova, J.J.T. Yates, J. Chem. Phys. 90 (1989) 4604.
[29] F. Zaera, J. Liu, M. Xu, J. Chem. Phys. 106 (1997) 4204.
[30] R. Imbihl, G. Ertl, Chem. Rev. 95 (1995) 697.
[31] C.E. Wartnaby, A. Stuck, Y.Y. Yeo, D.A.J. King, Chem. Phys. 102 (1995) 1855.
[32] A. Bourane, O. Dulaurent, D. Bianchi, J. Catal. 195 (2000) 406.
[33] M. Lynch, P. Hu, Surf. Sci. 458 (2000) 1.
[34] S.M. Dwyer, C.O. Bennett, J. Catal. 75 (1982) 275.
[35] J.H.B.J. Hoebink, J.P. Huinink, G.B. Marin, Appl. Catal. 160 (1997) 139.
[36] E.C. Su, W.G. Rothschild, H.C. Yao, J. Catal. 118 (1989) 111.
[37] T.A. Nijhuis, M. Makkee, A.D. van Langeveld, J.A. Moulijn, Appl. Catal. 164 (1997) 237.
[38] A. Bourane, D. Bianchi, J. Catal. 209 (2002) 123.